sciendo
Power Electronics and Drives
Volume 10(45), 2025 DOI: 10.2478/pead-2025-0006
Power Electronics and Drives

Further Investigations on Unconventional Slot Numbers in Concentrated Winding Electric Motors: Rotor Eccentricity and Conventional Methods for Torque Ripple Reduction

Research paper

Mike Königs*, Michael Harmel, Bernd Loehlein

Flensburg University of Applied Sciences, Flensburg, Germany

Received: 19 November, 2024; Accepted: 15 January, 2025

Abstract: Electric motors with unconventional slot numbers, especially prime numbers, have been shown to reduce cogging torque and torque ripple. Our previous study investigated an 8p12s servo motor topology known to be prone to cogging torque and torque ripple; in this publication, the research is expanded to a more robust 10p12s servomotor, including a comparison of the novel unconventional winding with a conventional topology with breadloaf magnets. Furthermore, Finite element method (FEM) simulations with rotor eccentricities are conducted to evaluate the impact of the novel topology on forces and torques under imperfect manufacturing. It is shown that the novel quadruple-layer topology with prime number of slots can effectively reduce cogging torque and torque ripple. Furthermore, the commonly used 10p12s servomotor topology can achieve similar performance using skewing and breadloaf permanent magnets. The novel topology is shown to be prone to torque ripple due to rotor eccentricity. Similar results to conventional concentrated windings can be achieved under imperfect manufacturing conditions.

Keywords: *synchronous motor • torque ripple • cogging torque • concentrated winding • permanent magnet*

1. Introduction

Previously, we discussed an unconventional winding system for concentrated windings with an arbitrary number of slots in terms of cogging torque reduction (Koenigs et al., 2025). Linear combinations of the *m* phases are chosen so that the complex magnetic scalar potential of the tooth is identical to the optimum based on sinusoidal magnetisation. The result is a quadruple layer that is winded with fractionally filled slots (Barbini and Tessarolo, 2019; Tessarolo et al., 2019; Totoki et al., 2022). When considered as a means of using a prime number of stator slots, this concept drastically reduces torque ripple under load and cogging torque. Cogging torque is the torque experienced when the motor is rotated without load in the stator windings due to the rotational change in reluctance. Torque ripple in general adds a current- and winding-dependent torque ripple component to the cogging torque and is therefore experienced under load. In the previous publication, the unconventional concentrated winding was compared to an 8-pole 12-slot concentrated winding motor. Although this 8p12s variant is used in the industry, it is not the industry standard for low-torque, ripple-concentrated winding motors (Azar et al., 2012; Jussila et al., 2007; Parsons, 2019). Additionally, state-of-the-art concentrated winding motors use breadloaf magnets, which was not the subject of the investigation in the previous study. This study compares an industry-standard 10p12s concentrated winding motor to a 10p13s concentrated winding motor with unconventional

* Email: mike.koenigs@hs-flensburg.de

winding. In addition to rotor skewing, breadloaf magnets are investigated. Skewing magnets (Dai and Lee, 2024; Liang et al., 2019; Petrov et al., 2020), breadloaf magnets (Hsieh and Hsu, 2005; Suriano-Sánchez et al., 2022), and other conventional measures (Brescia et al., 2020; Hu et al., 2018) reduce the cogging torque locally, while unconventional windings eliminate torque ripples based on a global concept. An investigation of eccentric rotors is conducted to confirm that the novel unconventional motor winding is prone to torque ripple due to static eccentricity.

2. Recap: Unconventional Slot Numbers in Concentrated Windings

This section is a short recapitulation of the design of unconventional slow-number electric motors with concentrated windings. Assuming a strictly theoretical sinusoidal magnetisation, the air gap field is sinusoidal, the teeth of the stator act as a window function, collecting the magnetic flux. The flux in a stator tooth is therefore sinusoidal as well. Ideally, the current in a concentrated coil in this stator would be in phase with the induced voltage. However, this is not always possible. With conventional symmetric three-phase systems, only three currents represented as complex vectors, spaced equally by 120°, are available. In two dimensions, two linearly independent vectors are sufficient to obtain any given vector by linear combination. Therefore, it is possible to find a linear combination of the three-phase currents so that the total current around the tooth matches the phase of the induced voltage. Only two phases are optimally used. The result is a concentrated quadruple-layer winding (Figure 1), although the concept applies to distributed windings as well. The unconventional quadruple-layer winding can be manufactured with industry-standard flyer coil winders on prefabricated insulation forms. The connection of multiple coils can be done with a standard contact ring. Winding two coils on each tooth and connecting them to the contact ring slightly increases the cost of those components. The other parts of the electric motor are unaffected by the winding design.

3. FEM Simulations

Four configurations were simulated using ANSYS Maxwell 2D software. The first three variants use an identical stator. One variant has a skewed rotor with four stages. To simulate the skewed model, multiple slices are simulated

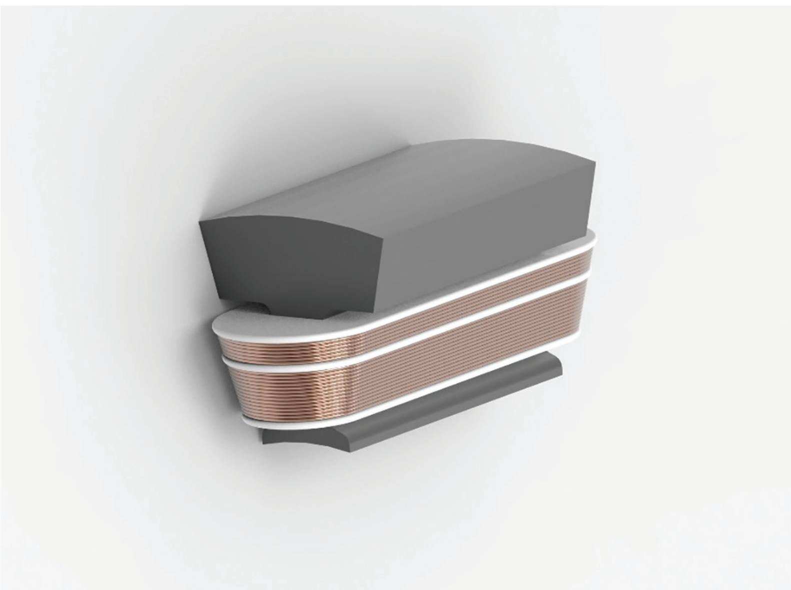

Figure 1. Two concentrated coils on a single tooth.

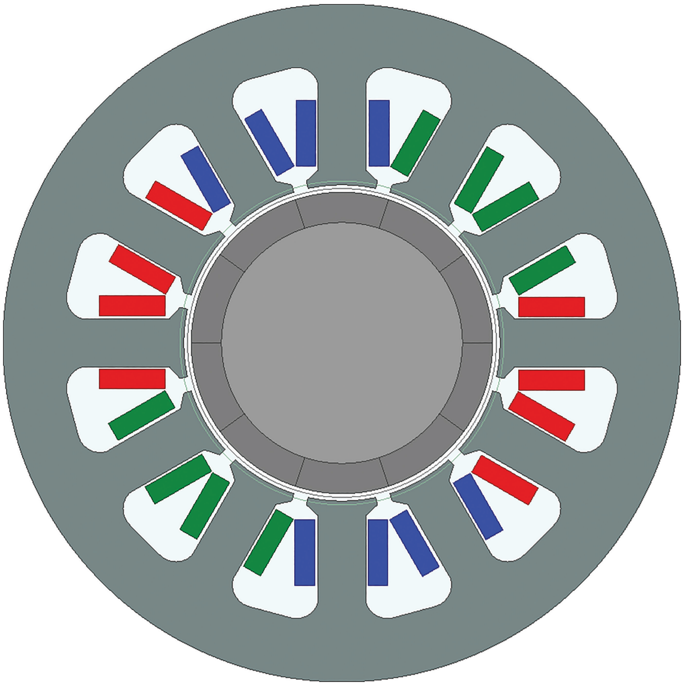

Figure 2. 2D cross section of a 10p12s machine with concentrated windings.

Table 1. Winding distribution of double layer 10p12s winding.

Tooth number	*U*	*V*	*W*	Sum
1	1	-	-	1
2	−1	-	-	1
3	-	−1	-	1
4	-	1	-	1
5	-	-	1	1
6	-	-	−1	1
7	−1	-	-	1
8	1	-	-	1
9	-	1	-	1
10	-	−1	-	1
11	-	-	−1	1
12	-	-	1	1

and then combined in the software package. The other variant has breadloaf magnets. All configurations are simulated using ideal sinusoidal currents in a balanced three-phase system. The cross section of the conventional concentrated winding 10p12s machine is shown in Figure 2. Each tooth has a single concentrated winding. The winding layout is given in Table 1. Usually, a winding distribution in each slot is given as a winding layout. In this case, the strand contribution to the coil around each tooth is used, as it is more intuitive to understand the unconventional winding.

Figure 3 shows the same stator as in the previous figure; however, the permanent magnets are replaced with breadloaf magnets.

Lastly, the geometry of the 13-slot 10-pole slot machine is given in Figure 4. Around each tooth, two coils are wound; the distribution of partial coils is not equal as depicted in the geometry. The distribution is fractional and optimized based on the ideal magnetic flux. In a real machine, rounding errors occur based on the integer number

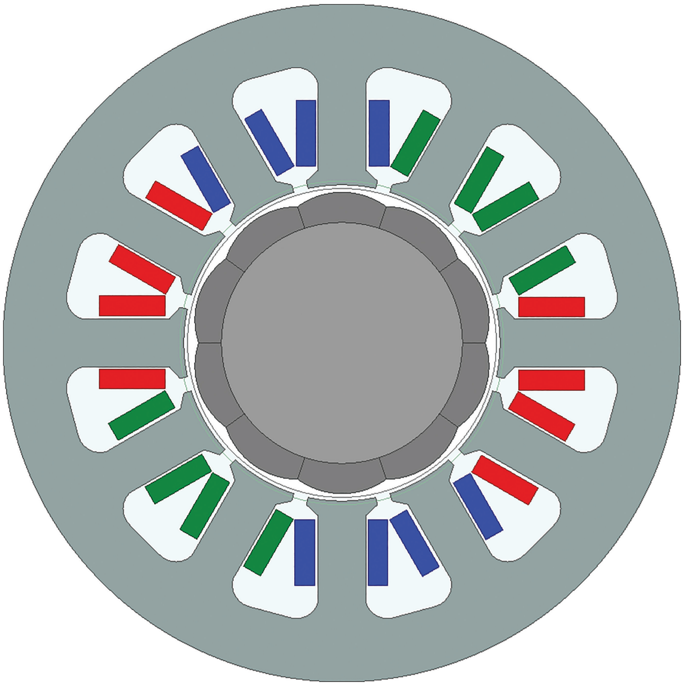

Figure 3. 2D cross section of a 10p12s machine with breadloaf magnets.

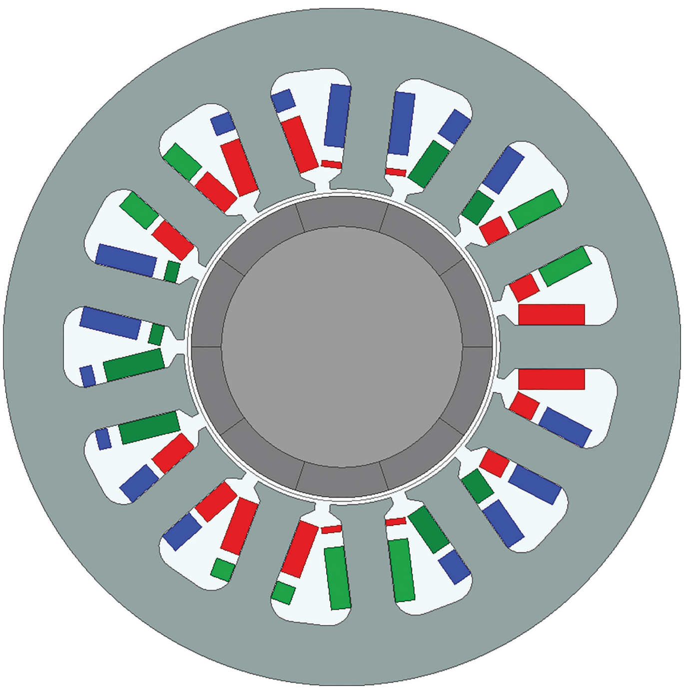

Figure 4. 2D cross section of a 10p13s machine.

of turns in the winding. The rounding error is different for every machine size and rated voltage. This is neglected in this work as an ideal current distribution is assumed. In this case, the induced voltages are almost balanced. The winding layout is given in Table 2. As can be seen in the sum column, the filling factor in each slot varies. In the lowest filled space, 87% of the conventional copper fill factor is used.

Table 2. Winding distribution of quadruple layer 10p13s winding.

Tooth number	*U*	*V*	*W*	Sum
1	0.87	-	-	0.87
2	−0.32	0.66	-	0.98
3	-	−0.60	0.39	0.99
4	0.08	-	−0.82	0.9
5	−0.72	-	0.24	0.96
6	0.53	−0.47	-	1
7	-	0.78	−0.16	0.94
8	-	−0.16	0.78	0.94
9	0.53	-	−0.47	1
10	−0.72	0.24	-	0.96
11	0.08	−0.82	-	0.9
12	-	0.39	−0.60	0.99
13	−0.32	-	0.66	0.98

Table 3. FEM simulation results.

Mean torque (Nm)	2.77	2.5	2.51	2.53
Voltage constant (Vrms/rad)	0.171	0.154	0.154	0.151
Cogging torque (Nm)	0.0524	0.0008	0.0126	0.0028
Relative cogging torque (%)	1.89	0.03	0.50	0.11
Torque ripple under load (Nm)	0.064	0.0035	0.0159	0.0065
Relative torque ripple under load (%)	2.30	0.14	0.63	0.26
Lateral force ripple (*N*)	0.025	0.016	0.201	0.879

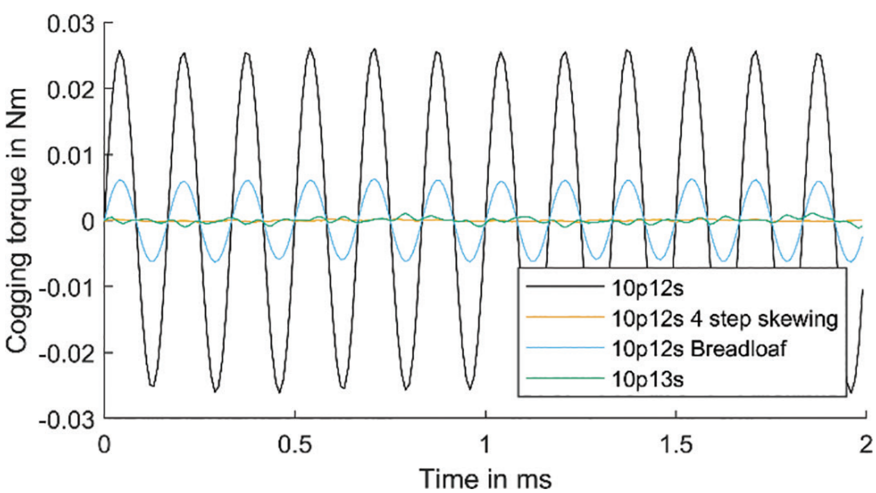

Figure 5. Cogging torque comparison.

Table 4. FEM simulation results for eccentric rotor (0.2 mm shift off centre).

Mean torque in Nm	2.77	2.5	2.51	2.53
Voltage constant in Vrms/rad	0.171	0.154	0.154	0.151
Cogging torque in Nm	0.0588	0.0013	0.016	0.0208
Relative cogging torque (%)	2.12	0.05	0.64	0.82
Torque ripple under load in Nm	0.0686	0.008	0.0212	0.024
Relative torque ripple under load (%)	2.48	0.32	0.84	0.95

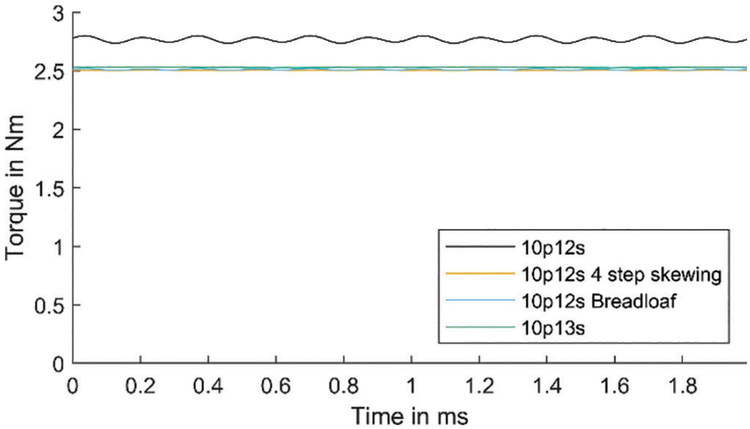

Figure 6. Torque comparison.

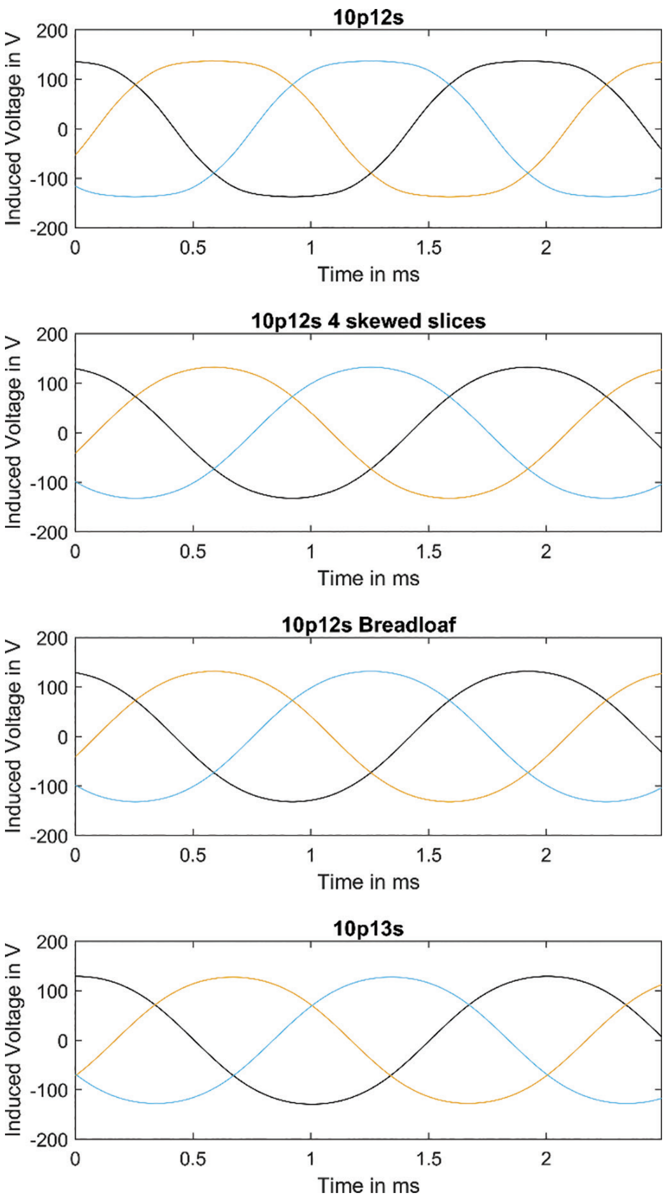

Figure 7. Induced voltage in no load operation.

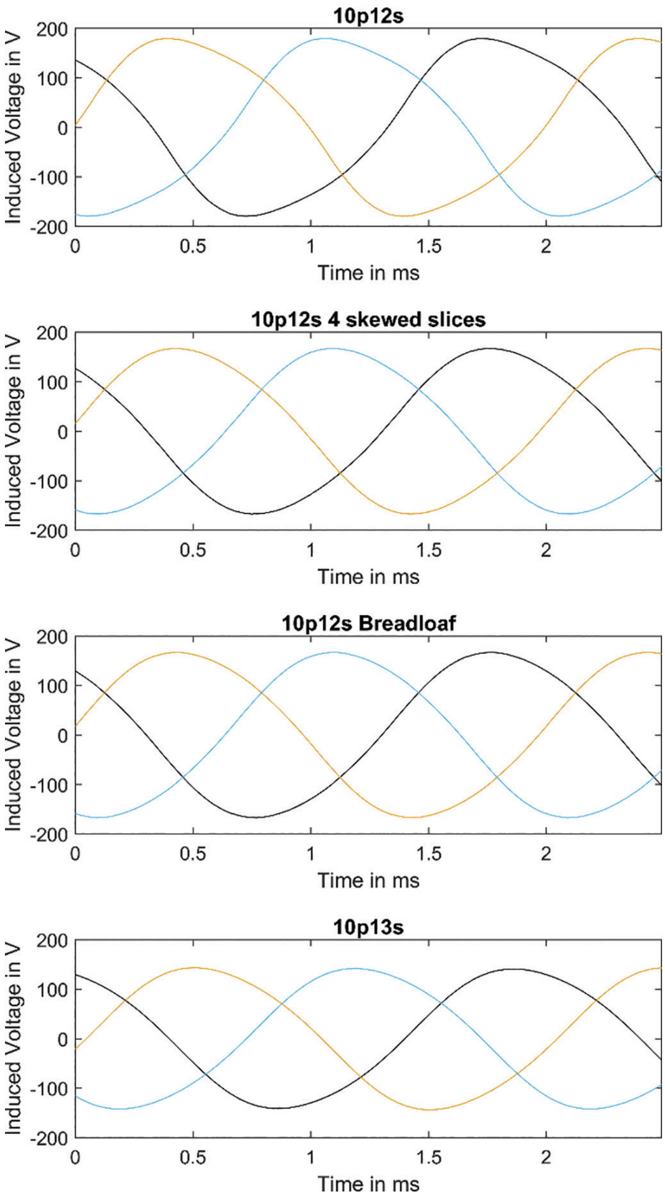

Figure 8. Induced voltage under 8 A/mm² load operation.

4. Results

4.1. Investigation of various rotor geometries

The original study was conducted to investigate the reduction in cogging torque and torque ripple in concentrated winding synchronous machines due to the use of a prime number as a number of slots. The Results are given in Table 3. Compared to the unskewed variant, all three adaptations show a significant reduction in torque ripple. Figure 5 shows the time-dependent behaviour of the cogging torque without load at 6,000 rpm. The exact values for the cogging torque are given in Table 4. Skewing with four stages reduced the cogging torque by 98%. An unskewed breadloaf magnet reduces the cogging torque by 73.5%. The unconventional winding reduces the cogging torque by 94.2%.

The reduction in torque ripple is also apparent in the torque under load, as shown in Figure 6. All torque ripple reduction methods exhibit a reduction in mean torque output. All methods are almost equal with around 90% of

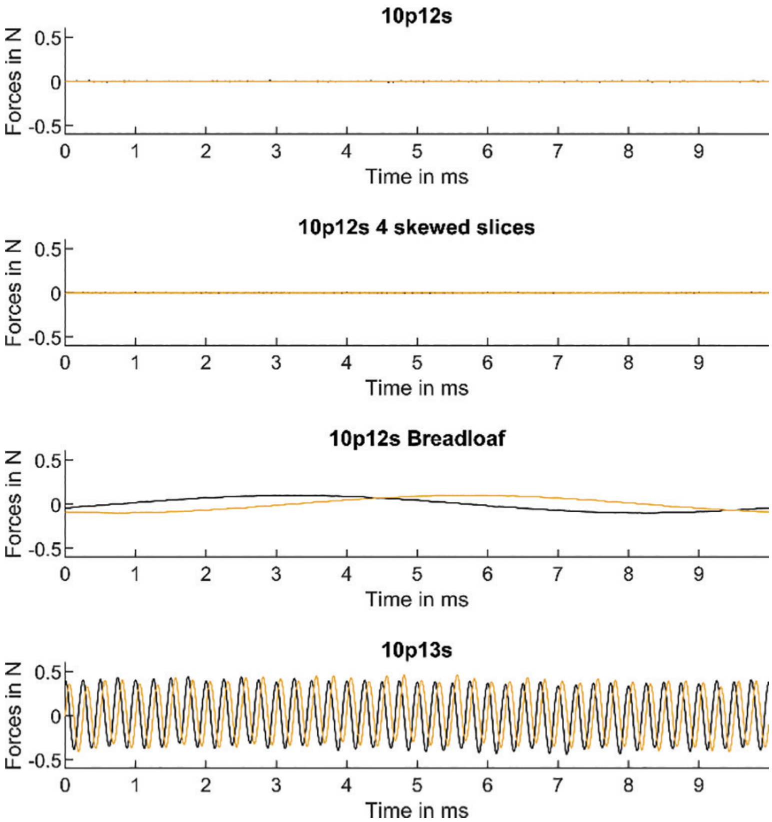

Figure 9. Radial forces under no load operation.

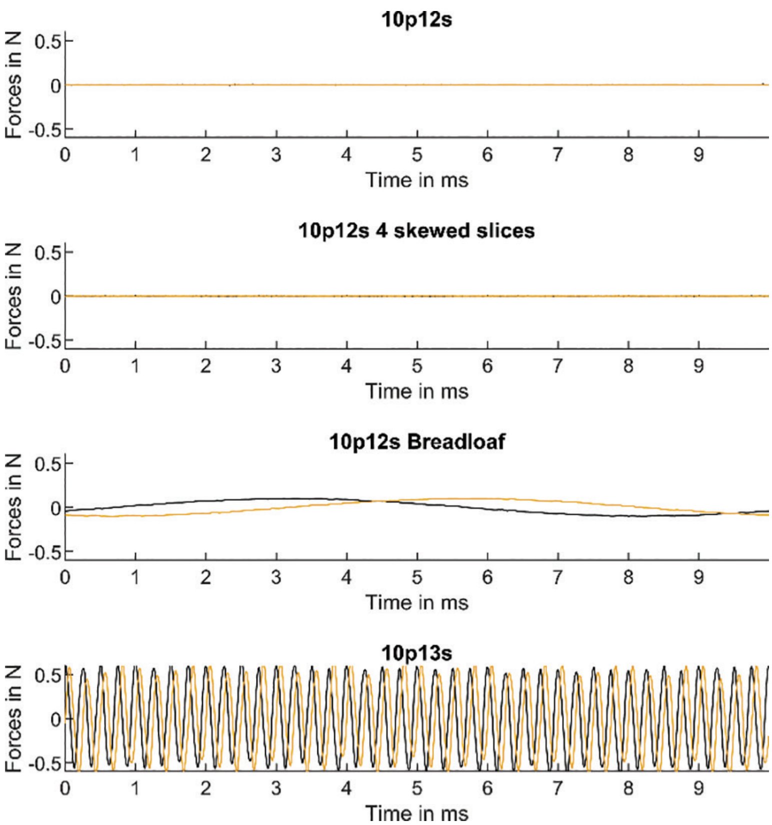

Figure 10. Radial forces under load operation.

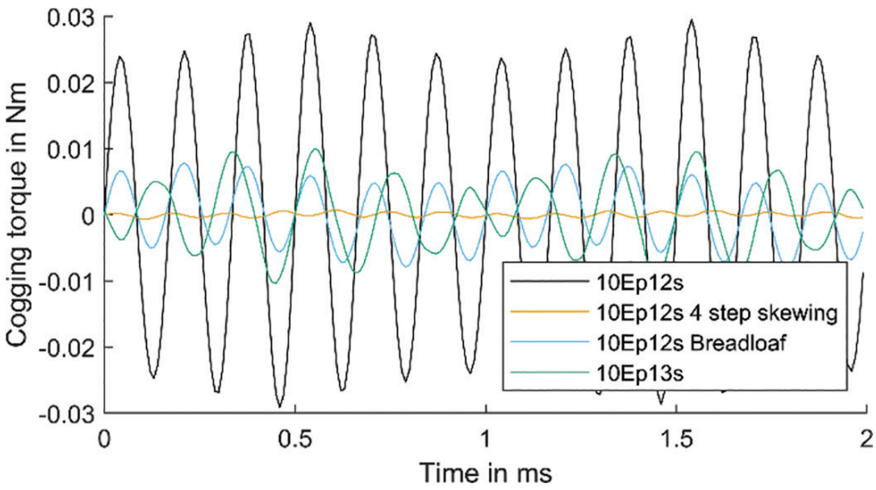

Figure 11. Cogging torque comparison with rotor eccentricity.

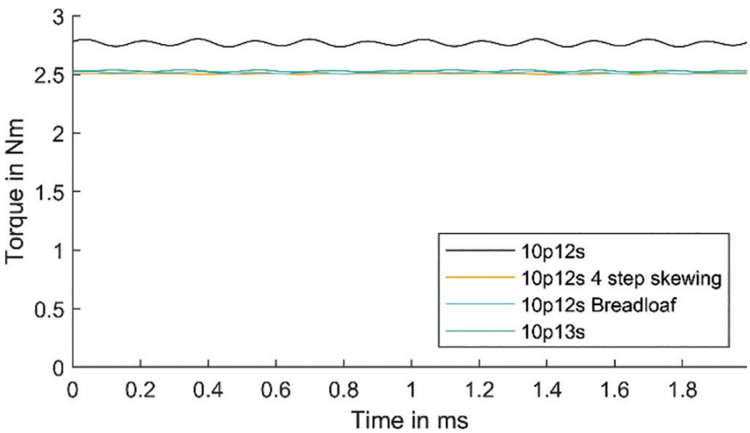

Figure 12. Torque comparison with rotor eccentricity.

torque generated. However, it should be noted that the unconventional winding uses 4.5% less copper than the other variants due to the reduced filling of certain slots.

Figure 7 shows the induced voltages under no load conditions per strand. As expected by the reduced output torque, the root mean square (RMS) values of the induced voltages decrease for all torque ripple reduction methodologies. The harmonic content is reduced in all three cases. The 10p13s variant has an almost balanced induced voltage system, even though the winding itself has no periodic symmetry regarding the strands. This is due to the large least common multiple (LCM) of the pole and slot numbers (Han, et al. 2006). A conventional winding distribution will experience similar unbalance due to the physical winding distribution and its associated leakage inductances for each turn.

Figure 8 shows the induced voltages under load conditions. A significant distortion of the voltage waveform is observed as a result of saturation effects.

Figures 9 and 10 display the radial forces on the rotor under no load and load conditions, respectively. While the conventional topology and the skewed rotor experience no radial forces whatsoever, the breadloaf variant and the unconventional design experience radial forces. The breadloaf variant experiences a very low-frequency force component, while the unconventional design has, by design, an unbalanced magnetic pull. Under load, the radial forces increase for the unconventionally wound machine.

4.2. Eccentricity of the rotor

The rotor of an electric motor is ideally directly centred in the bore of the stator, creating an ideal rotational symmetry. However, because of manufacturing tolerance, this is rarely the case. In many cases, the rotor has eccentricity; the

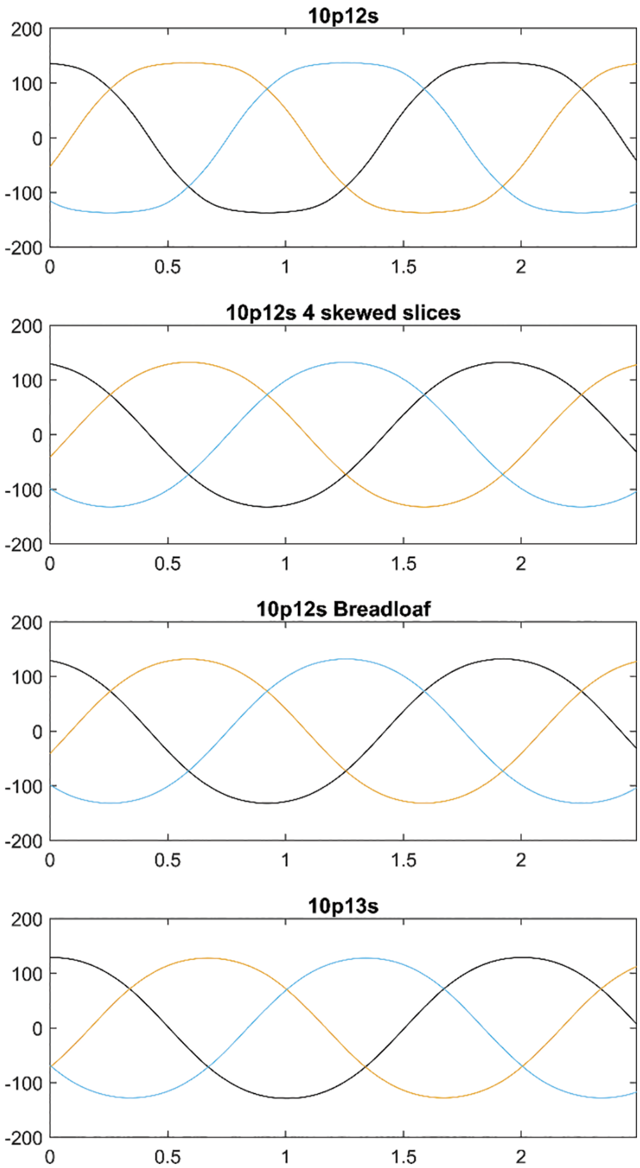

Figure 13. Induced voltage in no load operation with rotor eccentricity.

axis of the rotor does not align with the axis of the stator. This eccentricity can lead to distortions in the back EMF and torque ripples and can increase noise, vibration, and harshness. The impact of eccentricity depends on the motor parameters and topology (Li et al., 2017; Toporkov and Vialcev, 2017). In the following paragraphs, the effects of a misalignment of the rotor by 0.2 mm are investigated for the previously introduced motor topologies.

The torque ripple for an eccentric rotor is shown in Figure 11. Skewing with four stages reduces the cogging torque by 98%. Breadloaf magnets reduce the cogging torque with an eccentric rotor by 70%, and the unconventional winding reduces the cogging torque by 61%. The reduction in cogging torque by the breadloaf magnet is slightly reduced. The reduction in cogging torque of the unconventional winding design is significantly reduced.

The mean torque is independent of the eccentricity of the rotor in the observed cases. Figure 12 shows the torque in dependence on time.

Induced voltages under no load conditions are shown in Figure 13.

The induced voltages under load conditions are shown in Figure 14.

The radial forces due to eccentricity are shown in Figures 15 and 16 for no load and load conditions, respectively. The high-frequency component of the unconventional winding is now almost negligible compared to the static radial

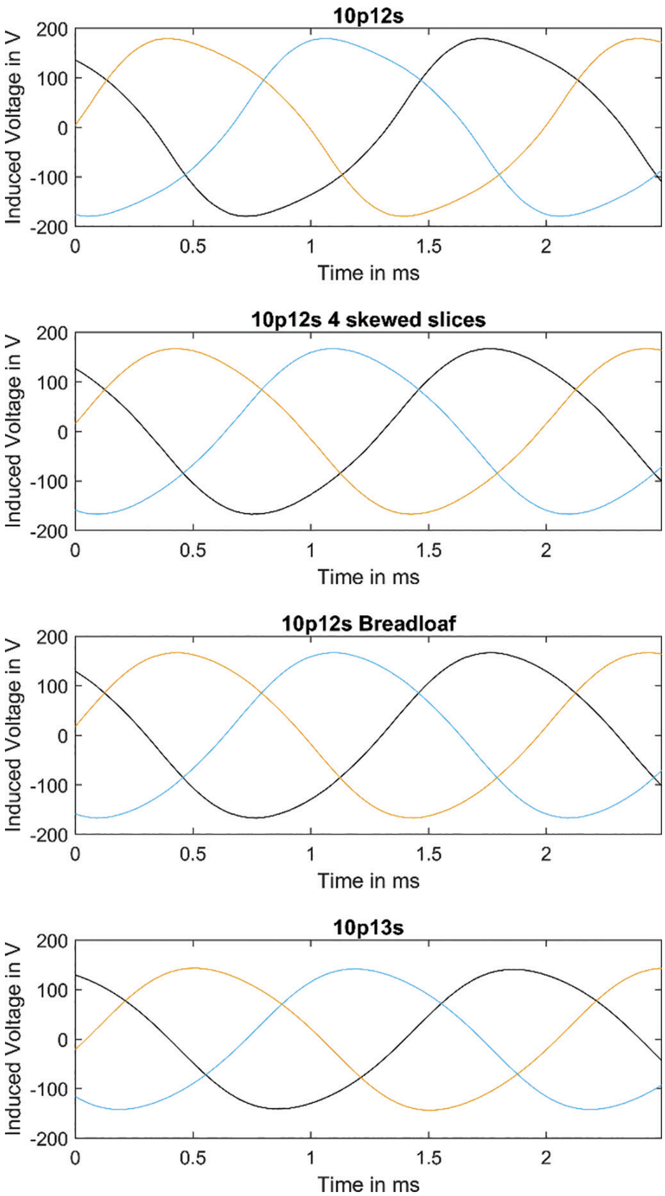

Figure 14. Induced voltage under 8 A/mm² load operation with rotor eccentricity.

force on the rotor. Furthermore, under load, all three 10p12s variants experience a fluctuation in radial force greater than the high-frequency component of the unconventional design.

5. Discussion

Compared to the 8p12s motor design investigated in our previous publication (Koenigs et al., 2025), the 10p12s design performs better in terms of torque ripple, both under load and under no load conditions. Breadloaf magnets significantly reduce torque ripple in the 10p12s variants. Four skew steps show the largest reduction in both cogging torque and torque ripple under load. When subjected to an axis misalignment of 0.2 mm, the 10p12s variants show a similar behaviour regarding the cogging torque and torque ripple reduction, as the measures of torque ripple reduction are based on a local reduction. The unconventional 10p13s variant, on the other hand, reduces torque ripple on a global scale. Therefore, it can be observed that the unconventional design is prone to torque ripple

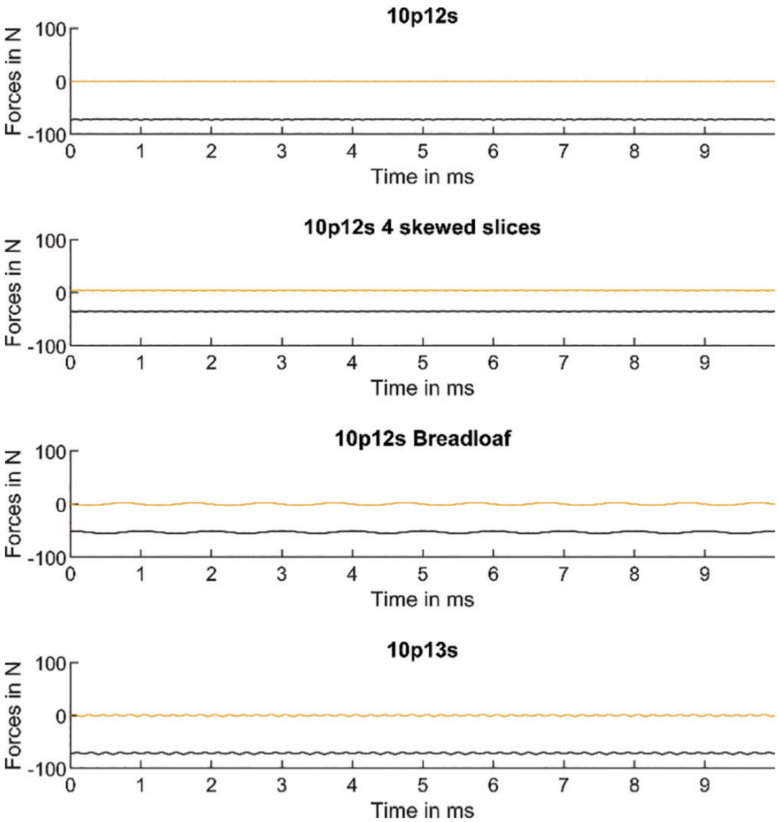

Figure 15. Radial forces under no load operation with rotor eccentricity.

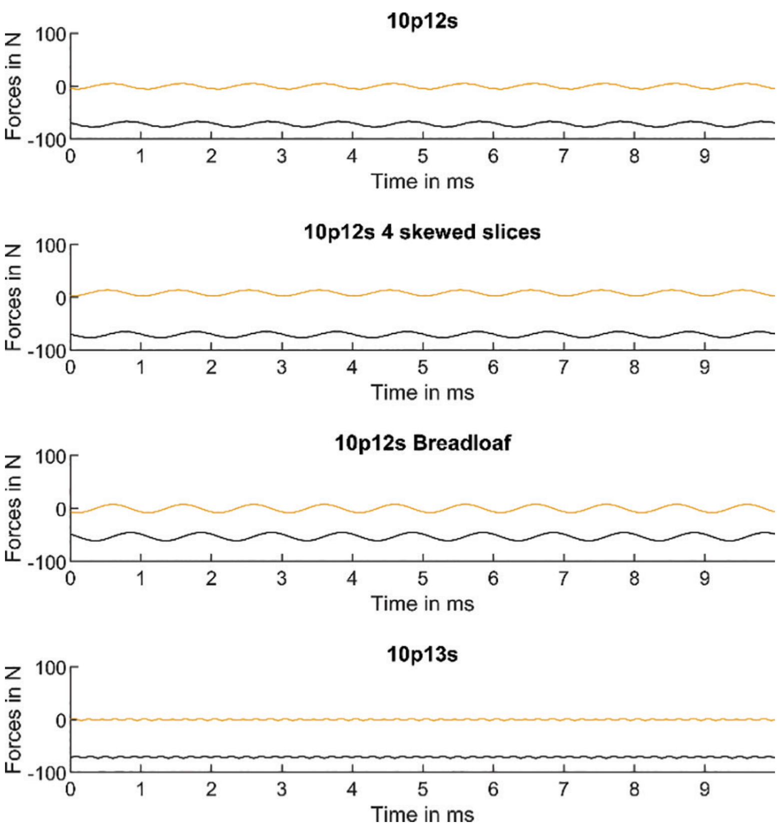

Figure 16. Radial forces under load operation with rotor eccentricity.

increase due to axis eccentricity. The increase in torque ripple in the unconventional winding design is similar to the torque ripple in the conventional breadloaf configuration.

6. Summary

Conventional concentrated windings synchronise machines with 10 poles and 12 slots without skewing, and 4 skewed stages and breadloaf magnets have been compared with an unconventional concentrated winding with 10 poles and 13 slots. The unconventional design significantly reduces the cogging torque and torque ripple. Similar results can be achieved with skewing and breadloaf magnets. The unconventional design has significant high-frequency radial force components. When subjected to rotor axis eccentricity, the cogging torque and torque ripple in the unconventional design increase significantly to levels of the unskewed breadloaf magnet in the 10p12s topology. Furthermore, under load, all three 10p12s variants experience a fluctuation in radial force greater than the high-frequency component of the unconventional design.

References

Azar, Z., Zhu, Z. Q. and Ombach, G. (2012). Influence of Electric Loading and Magnetic Saturation on Cogging Torque, Back-EMF, and Torque Ripple of PM Machines. *IEEE Transactions on Magnetics*, 48(10), pp. 2650–2658. doi: 10.1109/TMAG.2012.2201493

Barbini, N. and Tessarolo, A. (2019). *Concentrated winding electrical machine modelling, design, and optimization*. PhD. Thesis. *University of Trieste*. Available at: https://arts.units.it/retrieve/e2913fdd-03a8-f688-e053-3705fe0a67e0/Barbini_TesiPhD.pdf.

Brescia, E., Palmieri, M., Cascella, G.L. and Cupertino, F. (2020). Optimal tooth tips design for cogging torque suppression of permanent magnet machines with a segmented stator core. In: *2020 International Conference on Electrical Machines (ICEM)*. doi: 10.1109/ICEM49940.2020.9270968.

Dai, Y. and Lee, H. J. (2024). Torque Ripple and Electromagnetic Vibration Suppression of Fractional Slot Distributed Winding ISG Motors by Rotor Notching and Skewing. *Energies*, 17(19), p. 4964. doi: 10.3390/en17194964

Han, S. H., Jahns, T., Guven, M., Aydin, M. and Soong, W. (2006). Impact of maximum back-EMF limits on the performance characteristics of interior permanent magnet synchronous machines. In: *IEEE Industry Applications Society Annual Meeting (IAS)*. doi: 10.1109/IAS.2006.256804.

Hsieh, M. F. and Hsu, Y. S. (2005). An Investigation on the Influence of Magnet Arc Shaping Upon Back Electromotive Force Waveforms for the Design of Permanent-Magnet Brushless Motors. *IEEE Transactions on Magnetics*, 41(11), pp. 3949–3951. doi: 10.1109/TMAG.2005.854975

Hu, Y., Zhu, S., Liu, C. and Wang, K. (2018). Electromagnetic Performance Analysis of Interior PM Machines for Electric Vehicle Applications. *IEEE Transactions on Energy Conversion*, 33(1), pp. 199–208. doi: 10.1109/TEC.2017.2728689

Jussila, H., Salminen, P., Niemela, M. and Pyrhönen, J. (2007). Guidelines for designing concentrated winding fractional slot permanent magnet machines. In: *2007 International Conference on Power Engineering, Energy and Electrical Drives*, Setubal, Portugal, pp. 191–194. doi: 10.1109/POWERENG.2007.4380186.

Koenigs, M., Kremp, C., Holtorf, J., Harmel, M. and Loehlein, B. (2025). Improving Concentrated Winding Electric Drives Performance: Torque Ripple Reduction Through Non-Standard Stator Slot Numbers. Elektro & Informationstechnik Springer Verlag OVE Wien, Austria.

Li, Y., Liu, M., Kim, J.H. and Sarlioglu, B. (2017). Torque ripple reduction and mechanical tolerance analysis of a novel dual-stator 6/4 flux-switching permanent magnet machine. In: *2017 IEEE International Electric Machines and Drives Conference (IEMDC)*, Miami, FL, USA, pp. 1–8. doi: 10.1109/IEMDC.2017.8002329.

Liang J., Weisheng Jiang J., Yang Y., Al-Ani D., Bilgin B., Sathyan A. (2019). Torque ripple reduction for interior permanent magnet synchronous machines under load excitation by optimizing rotor skew angles. In: *2019 23rd International Conference on Mechatronics Technology (ICMT)*, Salerno, Italy, pp. 1–8. doi: 10.1109/ICMECT.2019.8932145.

Parsons, R. (2019). Selecting the best pole and slot combination for a BLDC (PMSM) motor with concentrated windings. *Things in Motion Blog*. Available at: https://thingsin-motion.blogspot.com/2019/01/selecting-best-pole-and-slot.html [Accessed 4 Sep. 2024].

Petrov, I., Hoffer, A. E. and Pyrhönen, J. (2020). Reduction of torque ripple in synchronous machines by quasi-skew-asymmetric rotor. In: *2020 International Conference on Electrical Machines (ICEM)*, Gothenburg, Sweden, pp. 298–304. doi: 10.1109/ICEM49940.2020.9270931.

Suriano-Sánchez, S. I., Ponce-Silva, M., Olivares-Peregrino, V. H. and De León-Aldaco, S. E. (2022). A Review of Torque Ripple Reduction Design Methods for Radial Flux PM Motors. *Eng*, 3, pp. 646–661. MDPI Electrical and Electronic Engineering doi: 10.3390/eng3040044

Tessarolo, A., Ciriani, C., Bortolozzi, M., Mezzarobba, M. and Barbini, N. (2019). Investigation into Multi-Layer Fractional-Slot Concentrated Windings with Unconventional Slot-Pole Combinations. *IEEE Transactions on Energy Conversion*, 34(4), pp. 1985–1996. doi: 10.1109/TEC.2019.2929950

Toporkov, D. and Vialcev, G. (2017). Impact of Equalizing Currents on Losses and Torque Ripples in Electrical Machines with Fractional Slot Concentrated Windings. *IOP Conference Series: Earth and Environmental Science*, 87, p. 032047. doi: 10.1088/1755-1315/87/3/032047

Totoki, E., Yamaguchi, S., Tanaka, T., Ito, K., Daikoku, A. and Morimoto, S. (2022). Torque Ripple Reduction for Permanent Magnet Motor Using New Configuration for Concentrated Windings. *IEEJ Journal of Industry Applications*, 11(3), pp. 531–537. doi: 10.1541/ieejjia.21001247